Simulation of Arctic and North Atlantic ocean water and ice seasonal characteristics by the INMIO-CICE coupled model

K V Ushakov[1,2,3], T B Grankina[1,2], R A Ibrayev[1,3,2,4], and I V Gromov[4]

[1] Hydrometeorological Research Centre of Russian Federation, 11-13 Bol'shoi Pedtechensky per., Moscow 123242, Russia
[2] P.P. Shirshov Institute of Oceanology RAS, 36, Nakhimovsky pr., Moscow 117218, Russia
[3] Institute of Numerical Mathematics RAS, 8, Gubkina str., Moscow 119333, Russia
[4] Moscow Institute of Physics and Technology, 9, Institutsky per., Dolgoprudny 141701, Russia

Email: ushakov@ocean.ru

Abstract. The first results of simulation of the seasonal variability of the Arctic and North Atlantic ocean waters and ice by a coupled model based on a full three-dimensional ocean dynamics model INMIO4.1 and a sea-ice model CICE5.1 are considered. The coupled model can be run on massively parallel computers under control of the Compact Modelling Framework CMF2.0. The numerical experiment is performed according to the CORE-II protocol with 1948 atmospheric forcing data. Possible causes of the deviation of the model solution from the ERA-20C reanalysis and WOA09 climatology are discussed.

1. Introduction

The Arctic region is an important territory both scientifically and economically. The Arctic Ocean (AO) is sometimes called the Arctic Mediterranean Sea or the Atlantic Ocean estuary. Due to its relatively small volume and long interface with the Atlantic Ocean, the processes taking place in the North Atlantic have a substantial influence on the Arctic Ocean. On the other hand, it is affected by relatively fresh Pacific Ocean waters coming through the Bering Strait.

The Arctic Ocean is bounded by Russia, Denmark, Iceland, Norway, Canada, and the USA. For the most part of the year it is used for sea cargo transportation and mineral and biological resources extraction. For the maintenance of economic activity it is important to have accurate and reliable operational information on the sea environment, including the ice conditions, which can be obtained by mathematical modelling. Seasonal numerical forecasting of the Arctic system is also very important because of the observed trends of regional warming, decrease in the sea ice area and volume and increase in the frequency of extremal weather condition events.

This paper is aimed at gaining the first experience on a coupled ocean-ice numerical simulation of the Arctic Ocean and model investigations of the mechanisms of intra-annual variability of the sea environment. Our numerical experiment is a calculation of the quasi-stable Arctic climatic system produced by cyclic annual variations of the atmospheric parameters and solar radiation taken from the CORE-II database [1] for the year 1948. The results obtained by the model are validated against the ERA-20C reanalysis [2] and WOA09 climatology [3,4] data.

In Section 2, ocean and ice models and a coupling technology are described. Section 3 shows the setup of the numerical experiment. Section 4 presents the results of the calculations. Section 5 contains conclusions and plans to develop the model.

2. Coupled model

The numerical experiment is performed with a coupled ocean-ice model at a nominal spatial resolution of 0.25°. The ocean component is a model called INMIO4.1 developed at the Institute of Numerical Mathematics of the Russian Academy of Sciences (INM RAS) and the Shirshov Institute of Oceanology (IO RAS). The sea ice is described by a model called CICE5.1 of the Los Alamos National Laboratory, USA. The coupled model is implemented for massively parallel computers under control of the Compact Modelling Framework CMF2.0 developed at INM RAS.

2.1 INMIO ocean model

The INMIO numerical model has been developed to investigate the general ocean circulation in a wide range of spatial and temporal scales. The full 3D PEM system of equations in the Boussinesq and hydrostatic approximations is implemented by a box-method for an arbitrary B-type horizontal grid and vertical z-axis. The water-air interface is described by free-surface conditions and explicit definition of heat, momentum, and water fluxes by the CORE atmospheric boundary layer bulk formulas [5]. At the solid lateral boundaries free slip and zero heat and salt flux conditions are imposed. To provide numerical stability, biharmonic filters are included in the momentum, heat, and salt transfer equations. The model has a built-in ice thermodynamics solver [6], which is also used in the calculations.

The momentum transfer term is approximated with a centered difference scheme. For the transport of heat, salt, and other tracers a flux-corrected transport scheme [7] is used. The water and tracer transport schemes are numerically consistent. In the time derivative approximation we use a leap-frog scheme, periodically applying an Euler step scheme for mutual relaxation of the computational modes. To use the computer resources effectively, the fast barotropic ocean processes are modelled separately from the baroclinic processes by solving a system of shallow water equations using a predictor-corrector scheme [8] with small time steps. The vertical turbulent mixing is parameterized by the Munk-Anderson scheme with convective adjustment of the unstable water columns. The background vertical viscosity and diffusion coefficients are 10^{-4} and 10^{-6} m^2/s, and the maximal values in regions with low Richardson numbers are 10^{-2} and 10^{-3} m^2/s, respectively. Except for the vertical mixing, all the processes are described by explicit numerical methods, which made it possible to effectively parallelize the program code [9]. A more detailed description of the model is presented in [10].

2.2 CICE ice model

The CICE sea ice model has been widely used by scientific groups all over the world. For instance, it was used in the AOMIP project [11]. The model defines the states of ice and snow in terms of their distribution functions $g(x,t,h)$ in time, geographical space, and thickness space. The description of ice includes several (by default, 5) thickness categories. The main prognostic variables for each category are the ice compactness (concentration), grid cell-mean ice and snow thickness, ice and snow internal energy, ice salinity, and surface temperature [12].

In this paper, the CICE model was run in a thermodynamic regime which includes modelling of the local processes of production, melting, and mutual conversion of ice and snow cover according to precipitation, diffusive heat conductivity, propagation of several radiation bands, heat exchange with the atmosphere and liquid water, evaporation and the corresponding latent heat flux, water and salt exchange with the ocean, and other processes with the exception of moving in space and internal stresses. The thermodynamics is modelled in a mushy approximation which describes the sea ice as a fresh ice medium containing brine pockets defining the distribution of salinity and enthalpy [13]. For the thermal conductivity, a bubble parameterization [14] is used. In addition to snow cover, the model

simulates the development of melt ponds as tracers including their drainage to the ocean. The solar radiation absorption is parameterized by the Delta-Eddington scheme.

2.3 Coupled model

The coupled INMIO-CICE ocean and ice model is implemented for massively parallel computer systems by means of the Compact Modelling Framework (CMF), which provides fully parallel interprocessor communications, multilevel data interpolation, and asynchronous I/O operations [15]. The CMF allows running an abstract coupled model consisting of an arbitrary number of components. Each of them, in turn, links in program libraries of a particular model (ocean, ice, atmosphere, land, etc.) and defines its own time cycle for solving the physical equations and periodical exchange of the two-dimensional data fields describing the interfaces with the other model components. In the exchange, these fields are remapped by the CMF from the source to the receiving grids.

In the coupled model, the data sent from the ice to the ocean includes ice concentration, ice-water stress components, fluxes of heat, salt, fresh water, and penetrating solar radiation. These quantities are summed over all ice categories. The ocean component sends to the ice component the fields of sea surface temperature, salinity, and velocity components, the surface tilt, and the freezing-melting potential. The latter is calculated before the data transmission and is equal to the coupling interval time mean heat flux necessary for the surface grid cell temperature to be brought to the freezing point. In the case where the potential is positive (i.e. the temperature is below the freezing point) the model instantly changes the water temperature to the freezing point, and then the ice model gradually calculates the corresponding changes in the ice volume and concentration, salt, and fresh water fluxes.

The atmosphere component is implemented by means of a CMF function which reads the forcing data from the NetCDF files and sends them to the ocean and ice components with remapping to the corresponding grids. The ocean and ice components receive the air temperature, specific humidity, and wind velocity components at a height of 10 m, downwelling short- and long-wave radiation, rain and snow intensity.

3. Numerical experiment setting

The purpose of the numerical experiment was to simulate the seasonal variability of the water circulation and ice of the Arctic Ocean under some defined annual variations of the atmospheric circulation. The experiment setting corresponds to the CORE-II protocol, which provides the daily mean downwelling radiation fluxes, monthly mean precipitation, continental runoff, and the diurnal cycle of atmospheric parameters (temperature, humidity, and wind) taken from the NCEP/NCAR reanalysis for the year 1948. The data also contains some modifications [16] for the ocean model to run correctly without the interactive atmospheric component. The monthly mean continental runoff is defined as the precipitation spread over the ocean surface close to the coasts and river estuaries. We have performed 5 model years of calculation with cyclic specified forcing data.

To avoid the model sea level drift, a surface water flux normalization condition is applied, i.e. the global mean value is subtracted from the total water flux (Prec – Evap + Runoff). The initial temperature and salinity conditions are taken from the annual mean WOA09 data, and the initial ocean current velocities are zero. The initial sea ice distribution fills the ocean north of 70° N with uniform 2m-thick ice. The ocean bottom topography is interpolated from the ETOPO5 database [17] without the internal continental water reservoirs and the Black Sea. The model time step is 10 min for the baroclinic and ice processes, and 20 s for the barotropic processes.

The horizontal model grid is three-polar [18] with poles in Siberia, North-Western Canada, and at the true geographic South Pole. The grid resolution in the spherical part (south of 60° N) is 0.25°. The grid cell dimensions vary from 28 km × 28 km at the equator to 6 km × 28 km on the Antarctic coast, 8 km × 17 km at the North Pole, and 11 km × 8 km along the continental coast of the Arctic Ocean. The vertical discretization includes 49 levels with steps from 6 m in the upper layer to 250 m in the

ocean depth. The ice model works in the area north of 42° and uses the same horizontal grid. Since the Antarctic is not the subject of the current study, it is handled with a simple built-in ice model [6] to reduce the computational expenses.

The space-variable horizontal heat and salt diffusion coefficient is taken proportional to the square root of the horizontal grid steps product, and the biharmonic diffusion coefficient is proportional to the 3rd power of this value. The simple and biharmonic background viscosity coefficients are scaled due to the grid steps in the same way. The corresponding diffusion values on the equator are 10^3 m^2/s and $-9 \cdot 10^9$ m^4/s. The horizontal viscosity coefficient is parameterized by the Smagorinsky method [19] with the coefficient $C^2=4$, and the background equatorial value is 10^3 m^2/s. For the biharmonic viscosity the coefficient is the same, and the background equatorial value is $-27 \cdot 10^9$ m^4/s. The shallow water equations use viscosity with a uniform coefficient of 100 m^2/s.

4. Results of the numerical experiment

Let us consider the last 5th year of the experiment and compare the model ice concentration field with the ERA-20C data for the months of the ice cover maximum and minimum, March and September. For the March ice concentration there is a good agreement of the model results with the reanalysis data (figures 1a and 1b). The only exception is the North Pacific region where the model shows slightly more ice. This confirms a hypothesis of [20] that to simulate the winter ice extent in the Northern Hemisphere it is generally sufficient to use a thermodynamic ice model.

The Arctic and North Atlantic ice extent in September is overestimated by the model, possibly because of the insufficient northward heat transport due to the low resolution, high model ocean viscosity, and the absence of southward ice transport, because the dynamic ice submodel was turned off, for instance, by the Labrador Current. On the other hand, the Pacific sector of the Arctic Ocean lacks ice, which may be explained by the incorrect simulation of the Bering Strait water transport or by peculiar features of the ocean weather in this year which cannot be simulated without taking into account the interannual variability. Since the 1990s there are many measurement data estimating this transport on a level of approximately 0.8 Sv northward, for instance, [21]. For the mid-20th century there are less data and their spread is larger, from 1 to 2-3 Sv [22]. Therefore, the estimate of 1.2 Sv by our model seems realistic. However, this question should be investigated in more detail to assess both the interdecadal variability and the accuracy of measurements and reanalysis data. Note that a close value of the Bering Strait transport (1.3 Sv) was obtained in [23] by the eddy-resolving INMIO model configuration with the ERA40 forcing.

Figure 1c shows the deviations of the modelled monthly mean temperatures from the corresponding fields of the ERA-20C reanalysis data for the chosen year. Inside the Arctic Ocean the deviations are rather small, since the surface temperatures are fixed by the freezing point equation. As for the neighboring basins, the large anomalies are close to the ice boundaries in the Labrador and Greenland Seas. Such seasonal conditions are very hard to simulate without an interactive atmospheric model. The mechanisms of model solution biases in this case are discussed in [16].

The March temperature distribution is greatly affected by the vertical mixing processes, since in this month it is usually most intensive. Consider the March upper mixed layer depth (MLD) based on the model solution and on the WOA09 data (figure 2). According to [24], let us define the MLD boundary as the depth at which the potential density (calculated from the monthly mean temperature and salinity) deviates from its surface value by 0.125 σ-units. The plotted depth range is limited to 1000 m. The model reproduces the MLD field reasonably well, except for the region of east-Atlantic mid-latitudes, possibly due to the weather peculiarities of the current year.

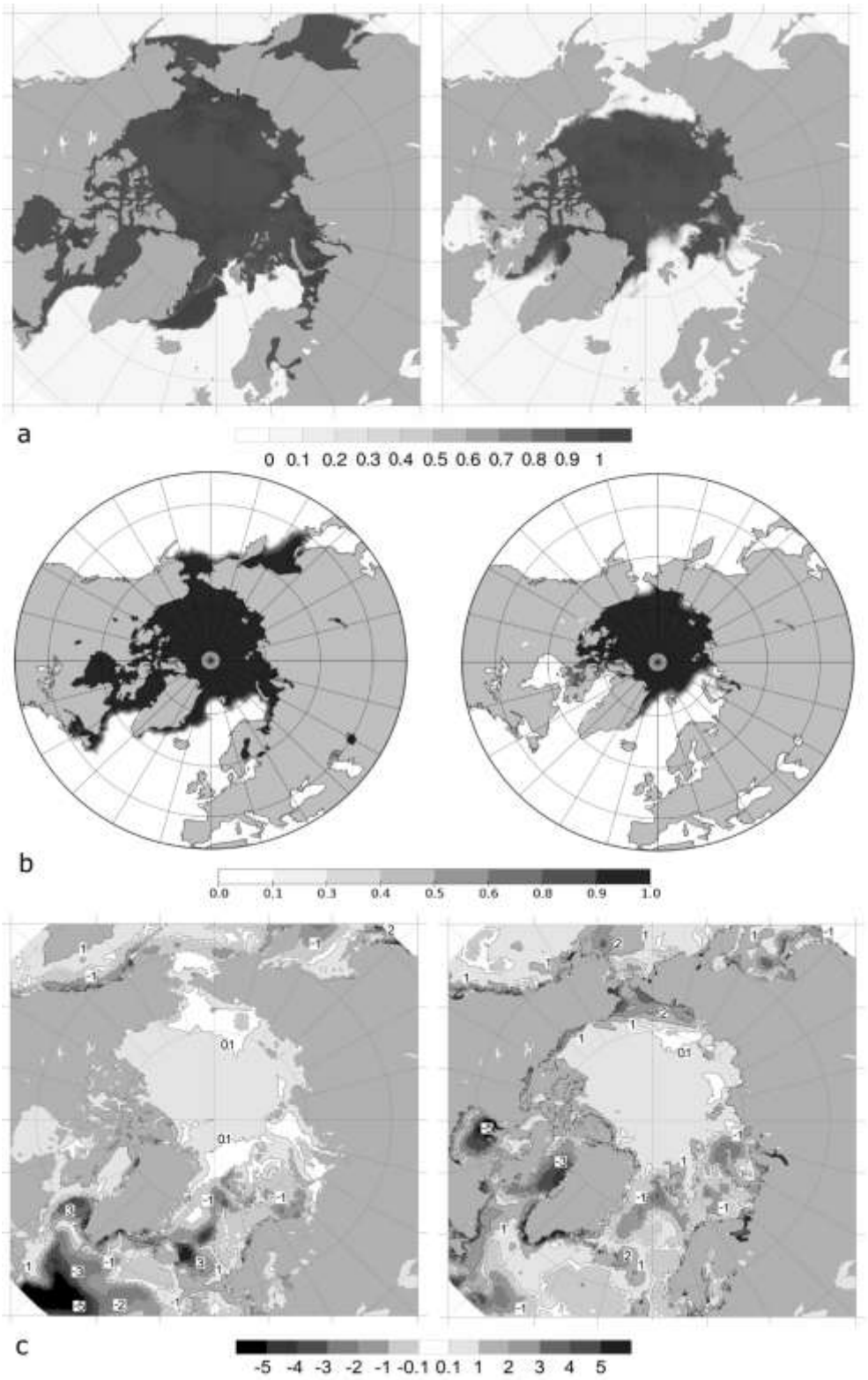

Figure 1. Monthly mean fields for March (left) and September (right): a – model ice concentration, b – ERA-20C ice concentration, c – model SST (ºC) deviation from ERA-20C.

The horizontal boundaries of the surface warm bias in the Labrador Sea are close to the boundaries of an area with deep mixing in the model solution and no such mixing in the WOA09 data. For example, in the north of the Labrador Sea (62ºN, 54ºW) the model convective adjustment penetrates up to the 25th model vertical level (550 m), while below this level the model and climatology data are close. The model MLD at this point is 2875 m, which coincides with the full model ocean depth. The climatological MLD is only 100 m, and the difference between the surface and bottom potential densities is 0.5 σ-units. Thus, it can be assumed that the March warm surface bias in the north of the Labrador Sea is caused by incorrect reproduction of the water stratification by the model. To correct such errors, a better vertical mixing parameterization should be used. A similar conclusion can be made from an analysis of the vertical T,S profiles off the south-west Svalbard coast, where the cold season convection leads to the development of a cold model bias persisting in summer.

On the other hand, a similar analysis of the vertical T,S distributions to the east and north-east of Iceland shows that vertical mixing is not directly associated with the development of a "dipole" surface temperature bias existing throughout the year. This effect is most pronounced in winter and is probably caused by the incorrect simulation of the complex structure of ocean currents near the ice edge and polar front [25].

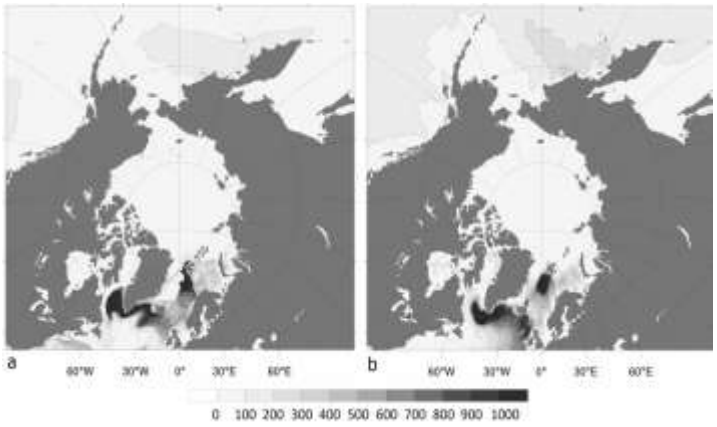

Figure 2. Ocean surface mixed layer depth in March (meters, a – based on model solution, b – based on WOA09 data).

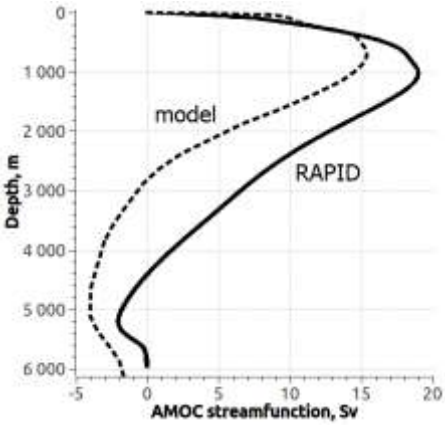

Figure 3. Vertical profile of the AMOC stream function at 26.5ºN based on model solution and RAPID data.

Figure 3 presents a comparison of vertical profiles of the Atlantic meridional overturning circulation (AMOC) stream function at 26.5ºN based on the model solution and RAPID 2004-2008 observation program data taken from [26]. The stream function is defined as the integral Atlantic northward water transport at the chosen latitude between the surface and the chosen depth. The model function differs from zero at the bottom, which corresponds to the contribution to AMOC from the Bering Strait transport, the continental runoff, and the surface water fluxes. The RAPID data include a spatially uniform corrective addition to the velocity field, such that its stream function is zero at the bottom.

Despite the different time periods and uncertainties in the RAPID data (velocity correction, use of the reference level method in open deep ocean), we see that the coupled model underestimates the meridional water transport (the stream function maximum is 15.4 Sv in the model solution and 18.6 Sv in the RAPID data).

The North Atlantic deep water (NADW) penetration depth, determined according to the zero isoline of the AMOC stream function, reaches about 3000 m, which is the value produced by most CORE-II models of [26] but less than that produced by the observational data. Therefore, the underlying Antarctic bottom water (ABW) occupies a larger depth range. The maximal ABW southward transport in the model solution (4 Sv at 5000 m) is correctly located on the vertical axis but

overestimated about 2 times; it lies at the upper boundary of the model results range in [26]. Since the main source of NADW are dense and cold Nordic Seas' waters overflowing the Greenland-Scotland Ridge [27], to improve its simulation it may be necessary to use a parameterization of the overflowing process.

Finally, we consider the mechanism of development of the September warm bias in the Chukchi Sea. Figure 4 shows the annual variations of the surface ocean parameters at (69ºN, 170ºW). According to the CICE conventions, fluxes are defined per unit area of ice, and ice and snow thicknesses are grid cell-averaged.

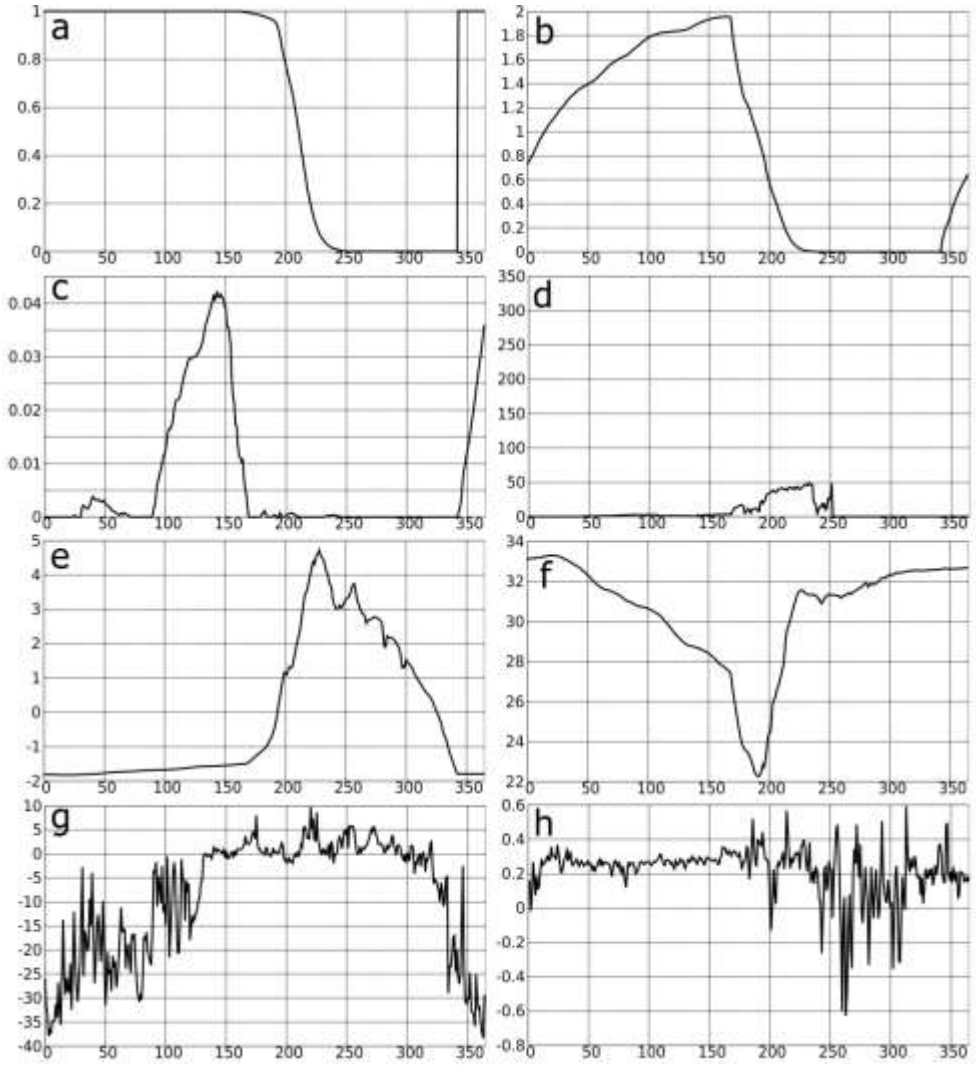

Figure 4. Annual variations of surface ocean parameters at (69ºN, 170ºW): a – ice concentration, b – ice thickness (m), c – snow thickness (m), d – ice-penetrating shortwave radiation (W/m^2), e – sea surface temperature (°C), f – sea surface salinity (psu), g – air temperature (°C). In the narrowest section of the Bering Strait: h – section-averaged northward surface velocity (m/s).

It can be seen that the dramatic change in the surface ocean characteristics in the chosen location is on the 170th day of the year, when the sea surface temperature exceeds the freezing point and the ice concentration and thickness start to decrease quickly. Before that time the ocean is covered with ice and snow, and the ocean surface heat and radiation fluxes are close to zero. Thus, we may conclude that the gradual pre-170th day heating of the ocean surface layer may be caused by warm Pacific water

whose transport in the Bering Strait is relatively stable in this period. A contribution can also be made by the snow cover melting, which starts on the 140th day, when the air temperature rises above zero and leads to an increase in the solar radiation absorbed by the ice and ocean water. This process is accompanied by gradual ocean freshening, which speeds up when the ice starts melting and stops on the 190th day, when the Bering Strait current slows down and becomes unstable. Thus, the Chukchi Sea ice discharge in September can be qualitatively explained by two successive processes: 1) gradual Pacific water heating and penetrating solar radiation due to melted snow cover; 2) start of fast ice melting and open water heating by solar radiation. In [28] it is pointed out that precipitation plays an important role in the ocean freshening in this period, which deserves further investigation.

5. Conclusions

The work has yielded the first results of a calculation of the Arctic Ocean characteristics using a coupled simulation by the INMIO-CICE model with a spatial resolution of 0.25°. The 5-year numerical experiment is the first important step in the development of a modern coupled ocean-ice model. Its results show that on the space and time scales considered the coupled model can reproduce the Arctic Ocean thermohydrodynamic variability qualitatively well. The causes of the main model solution biases from the "real" ERA-20C reanalysis data and WOA09 climatology have been identified. The ice-ocean model can be used as a powerful tool for the investigation of large-scale circulation and regional forecasts. Further work will include tuning of the model in an eddy-permitting regime with ice dynamics, improvement of the parameterizations, and use of a higher resolution.

Acknowledgements

This work was supported by the Russian Science Foundation (project no. 14-37-00053) and performed at the Hydrometeorological Research Centre of the Russian Federation.

References

[1] Large W and Yeager S 2009 The global climatology of an interannually varying air–sea flux data set *Clim. Dyn.* **33** (2-3), 341-364.
[2] Poli P et al 2016 An Atmospheric Reanalysis of the Twentieth Century *J. Climate* **29**, 4083–4097.
[3] Locarnini R A et al 2010 World Ocean Atlas 2009, Volume 1: Temperature. S Levitus Ed. *NOAA Atlas*, 184 pp.
[4] Antonov J I et al 2010 World Ocean Atlas 2009, Volume 2: Salinity. S Levitus Ed. *NOAA Atlas,* 184 pp.
[5] Large W and Yeager S 2004 Diurnal to decadal global forcing for ocean and sea-ice models: the data sets and flux climatologies *NCAR Technical Note: NCAR/TN-460+STR* (CGD Division of the National Center for Atmospheric Research) 105 pp.
[6] Schrum C and Backhaus J 1999 Sensitivity of atmosphere-ocean heat exchange and heat content in North Sea and Baltic Sea. A comparative Assessment *Tellus* **51**A 526-549.
[7] Zalezak S T 1979 Fully multidimensional flux-corrected transport algorithm for fluids *J. Comput. Phys.* **31** 335-362.
[8] Griffies S M 2015 Elements of the Modular Ocean Model (MOM) (2012 release with updates) *GFDL Ocean Group Technical Report* **7** 645 pp.
[9] Kalmykov V V 2013 Program complex for numerical modelling of the coupled system of ocean-atmosphere on massively parallel computers, PhD thesis (Moscow, INM RAS, in Russian).
[10] Ibrayev R A, Khabeev R N and Ushakov K V 2012 Eddy-resolving 1/10° model of the World Ocean *Izv. Atmos. Ocean. Phys.* **48(**1) 37-46.
[11] Johnson M et al 2012 Evaluation of Arctic sea ice thickness simulated by Arctic Ocean Model Intercomparison Project models *J. Geophys. Res.* **117** C00D13.
[12] Hunke E C et al 2015 CICE: the Los Alamos Sea Ice Model Documentation and Software

User's Manual Version 5.1 (Los Alamos National Laboratory).
[13] Feltham D L, Untersteiner N, Wettlaufer J S and Worster M G 2006 Sea ice is a mushy layer *Geophys. Res. Lett.* **33** L14501.
[14] Pringle D J, Eicken H, Trodahl H J and Backstrom L G E 2007 Thermal conductivity of landfast Antarctic and Arctic sea ice *J. Geophys. Res.* **112** C04017.
[15] Kalmykov V V Ibrayev R A 2013 A framework for the ocean-ice-atmosphere-land coupled modeling on massively-parallel architectures *Vychislitel'nye Metody i Programmirovanie* **14** 88-95.
[16] Griffies S M et al 2009 Coordinated ocean-ice reference experiments (COREs) *Ocean modelling* **26(**1-2) 1-46.
[17] ETOPO5 1988 Data Announcement 88-MGG-02. Digital relief of the Surface of the Earth (NOAA, National Geophysical Data Center. Colorado).
[18] Murray R J 1996 Explicit Generation of Orthogonal Grids for Ocean Models *J. Comp. Phys.* **126**(2) 251-273.
[19] Griffies S M and Hallberg R W 2000 Biharmonic Friction with a Smagorinsky-Like Viscosity for Use in Large-Scale Eddy-Permitting Ocean Models *Mon. Wea. Rev.* **128** (8) 2935–2946.
[20] Ushakov K V, Ibrayev R A, Kalmykov V V 2015 Simulation of the World Ocean climate with a massively parallel numerical model *Izv. Atmos.Ocean. Phys.* **51**(4) 362-380.
[21] Roach A T et al 1995 Direct measurements of transport and water properties through the Bering Strait *J. Geophys. Res. Oceans* **100(**18) 443–458.
[22] Bloom G L 1964 Water transport and temperature measurements in the eastern Bering strait, 1953–1958 *J. Geophys. Res.* **69** (16) 3335–3354.
[23] Khabeev R N 2013 Features of the North Atlantic water circulation in the 3-dimensional eddy-resolving World Ocean model PhD thesis (Moscow, MSU, in Russian).
[24] Monterey G and Levitus S 1997 Climatological cycle of mixed layer depth in the world ocean. (U.S. government printing office, NOAA NESDIS, Washington, DC) 5 pp.
[25] Wanamaker A D et al 2012 Surface changes in the North Atlantic meridional overturning circulation during the last millennium *Nat. Commun.* **3** 899.
[26] Danabasoglu G et al 2014 North Atlantic Simulations in Coordinated Ocean-ice Reference Experiments phase II (CORE-II). Part I: Mean States *Ocean Modelling* **73** 76-107.
[27] Dickson R and Brown J 1994 The production of North-Atlantic deep waters – sources, rates, and pathways *J. Geophys. Res. Oceans*. **99** (C6) 12319–12341.
[28] He Y et al 2015 Observed features of temperature, salinity and current in central Chukchi Sea during the summer of 2012 *Acta Oceanol. Sin.* **34** (5) 51–59.